Synthesis and Vibrational Spectroscopy of 1,1,2,2-Tetrafluoroethane and Its $^{13}C_2$ and d_2 Isotopomers†

Norman C. Craig,* Jessica I. Chuang, Christiana C. Nwofor, and Catherine M. Oertel

Department of Chemistry, Oberlin College, Oberlin, Ohio 44074

Received: February 7, 2000; In Final Form: March 16, 2000

The $^{13}C_2$ and d_2 isotopomers of 1,1,2,2-tetrafluoroethane (TFEA) have been synthesized. Raman spectra of these new species have been recorded, and infrared spectra of all three isotopomers, including some regions with high-resolution at −100 °C, have also been recorded. Guided by recently published calculations of frequencies and infrared intensities and the new spectra, we have revised the previous assignments of fundamentals for the two rotamers of the normal species of TFEA. Assignments of the fundamentals for both rotamers of the $^{13}C_2$ and d_2 isotopomers are proposed. The anti rotamer is the more abundant species in the gas phase and, to a lesser extent, in the liquid phase and the only species in the crystal phase. Thus, the assignments of the anti rotamer of all three isotopic species are complete and supported by isotope product rules, but the assignments for the gauche rotamers are incomplete. Estimates of the missing frequencies for the gauche rotamer of the normal species are supplied.

Introduction

The two rotamers of 1,1,2,2-tetrafluoroethane (TFEA) are of interest as part of the study of the puzzling gauche effect. The rotamers of the less-substituted 1,2-difluoroethane exhibit the gauche effect. Thus, the gauche rotamer of 1,2-difluoroethane has a lower energy than the anti rotamer despite the closer approach of the two highly electronegative fluorine atoms in the gauche rotamer.[1,2] The lower energy of the gauche rotamer of 1,2-difluoroethane is affirmed in high-level ab initio calculations by Muir and Baker.[3] Wiberg has provided a qualitative rationalization for this result in terms of a *de*stabilization of the anti rotamer by adverse bond bending in the CC σ bond.[4] Engkvist, Kalstrom, and Widmark have used what amounts to a four-center interaction involving the FCCF framework to rationalize the gauche effect through a stabilization of the gauche rotamer.[5] Applying either of these qualitative arguments predicts that the rotamers of TFEA should be an even more striking example of the gauche effect with the gauche rotamer having the lower energy. Yet, experimental evidence shows that the anti rotamer has a lower energy by about 4.9 kJ/mol in the gas phase.[6] Ab initio calculations by the ACM-density functional method and by the MP2 method concur with the sign and magnitude of this experimental result.[3,7] They give 5.4 and 6.9 kJ/mol, respectively, for the energy of the gauche rotamer relative to the anti rotamer. In addition, Epiotis has used a valence bond argument to rationalize the lower energies of the gauche rotamer in 1,2-difluoroethane and the anti rotamer in TFEA.[8]

We have previously applied the analysis of the rotational structure in high-resolution infrared spectra to finding the complete structure of the nonpolar anti rotamer of 1,2-difluoroethane.[2] This structure shows significant changes in bond lengths and bond angles in comparison with the structure of the gauche rotamer, which was found by microwave spectroscopy.[9] Such geometric differences between rotamers have the potential for evaluating qualitative theories of the gauche effect and for evaluating the quality of ab initio calculations.

The long-range goal of the present investigation is to find the complete structures of both rotamers of TFEA. A fine start was made at NIST and PNL by Stone, Philips, Fraser, Lovas, Xu, and Sharpe, who obtained ground-state rotational constants for both rotamers.[10] The rotational constants for the anti rotamer came from the analysis of the rotational structure in a band in the high-resolution infrared spectrum, observed in a jet-cooled beam with a diode laser. The rotational constants of the gauche rotamer came from a microwave study. To complete the structural analysis, high-resolution spectra of isotopic modifications of TFEA are needed. The present study is on the synthesis of the needed isotopomers and the analysis of their medium-resolution vibrational spectra as a prelude to the high-resolution investigations.

Two studies have been made of the vibrational fundamentals of the two rotamers of the normal form of TFEA. The first was by Klaboe and Nielsen.[11] A more extensive study was done by Kalasinsky, Anjaria, and Little with improved instrumentation.[6] The second investigation led to a revised assignment of the fundamentals of the two rotamers. In the meantime, two ab initio studies of the vibrational frequencies have been published.[7,12] The work by Papasavva, Illinger, and Kenny,[7] which used higher-level theory, provides a good basis for reviewing the assignment of the vibrational fundamentals. As part of their study, they computed infrared intensities as well as frequencies. In general, these calculations are consistent with the Kalasinsky assignment but, coupled with information from the high-resolution infrared spectrum and from the investigation of two isotopomers, we propose revisions in the assignments of vibrational fundamentals of both rotamers.

A method had to be devised to synthesize the isotopomers of TFEA. We thought that the reaction of silver difluoride with 1,1,2,2-tetrabromoethane (TBrEA) might succeed, as had a similar reaction for making 1,2-difluoroethane from 1,2-dibromoethane.[2] Indeed, AgF_2 works but at a temperature well above the room-temperature reaction conditions that were used in the

† Part of the special issue "C. Bradley Moore Festschrift".

10.1021/jp0004967 CCC: $19.00
Published on Web 05/11/2000

reaction with 1,2-dibromoethane. At an intermediate temperature of 80 °C, AgF_2 converts TBrEA into 1,1-dibromo-2,2-difluoroethane. A temperature of 150 °C is needed to complete the formation of TFEA. TFEA was first made in the 1930s by Henne and Midgley by reaction of HgF_2 with TBrEA in a metal reactor at elevated temperatures and pressures.[13] We regard AgF_2 as a more easily used and safer reagent for small-scale synthesis. AgF_2 is an underutilized reagent for fluorinations. Appropriate commercially available acetylenes serve as starting materials for making the d_2 and $^{13}C_2$ isotopic species. Bromine addition to acetylene-d_2 and to acetylene-$^{13}C_2$ provides the needed TBrEA isotopomers.

TFEA is also of interest as a possible replacement for Freons in refrigeration systems. Having good spectroscopic information about this substance is important for monitoring its presence and fate in the atmosphere.[14]

Experimental Section

Synthesis and Characterization. Normal TFEA (bp −20 °C) was purchased (PCR) and used in spectroscopic studies without purification.

TBrEA-d_2 was made photochemically with an essentially 1:2 molar ratio of acetylene and bromine in a 1.1-L flask equipped with a standard-taper joint and a vacuum stopcock on the top end and a 19/38 standard-taper joint with a mated tube on the bottom end. The flask was greased with Krytox grease (Dupont) and contained some short lengths of Teflon tubing to aid in mixing gases. 175 Torr of acetylene-d_2 (Cambridge Isotope Labs, 99% D) was measured into the evacuated 1.1-L flask and then condensed in a holding flask. 173 Torr (fixed by the v.p. at 20 °C) of bromine (Fisher, ACS reagent) was measured into the 1.1-L flask and stored in a third flask. A second 173-Torr of bromine was measured into the 1.1-L flask. The two portions of bromine were condensed at liquid-nitrogen temperature in the very bottom of the tube at the bottom of the evacuated flask, and the acetylene-d_2 sample was condensed higher up in the tube out of contact with the bromine. The flask, with its contents still condensed in the bottom, was taken into near darkness, slowly warmed and shaken well. Initially a small flashlight was used for illumination as shaking was continued. Then, over a period of 35 min, the flask was slowly brought toward full fluorescent lighting. To complete the reaction, the flask was left for several hours near a daylit window. The rather involatile TBrEA-d_2 product, which collected as droplets on the walls of the flask, was chased into the detachable tube at the bottom of the flask by cooling the tube in liquid nitrogen and using a heat gun. After warming the product to room temperature, air was admitted to the reaction flask. The identity of TBrEA-d_2 was confirmed by ^{13}C NMR ($\delta = 46.56$ ppm, equal intensity triplet with $J_{CD} = 27.6$ Hz) and deuterium NMR (singlet, $\delta = 5.92$ ppm).

TFEA-d_2 was prepared by reaction of silver difluoride with TBrEA-d_2. The reaction was run in a 100-mL flask equipped with some short pieces of Teflon tubing and a 19/38 inner ground joint, which was attached through this joint to a stopcock and another ground joint. Silicone grease, which withstands elevated temperatures, was used. In a reaction, 3.50 g (24 mmol) of AgF_2 (Aldrich) was transferred into the reaction flask in a nitrogen-purged dry bag. On the vacuum system the nitrogen was pumped away, and the AgF_2 was heat-gunned repeatedly until a new heating gave a pressure rise of only a few microns. This rigorous "drying" of AgF_2 is key to controlled reactions with this reagent. With nitrogen purge techniques a serum bottle cap was put on the reaction flask in place of the stopcock adapter, 0.23 mL (2.0 mmol) of TBrEA-d_2 was injected with a syringe, and the stopcock adapter was replaced. Nitrogen was pumped away on the vacuum system. The mixture was shaken and put into an oven at 150 °C but with the stopcock kept outside the heated region. Every 15 min over a 3-hr period the flask was removed from the oven and shaken. After the heating period, the bottom of the flask was cooled in liquid nitrogen, and noncondensable gases were pumped away. To remove byproduct CO_2, Br_2, and SiF_4, the crude product was passed through a column packed with Ascarite II (Thomas Scientific) which had been dampened by drawing room air through the column before use. The sample was dried by passing it through a column containing P_2O_5 dispersed on glass wool. TFEA-d_2 was isolated by preparative gas chromatography in two stages. The first stage was on a 1-m column packed with 10% (w/w) tricresyl phosphate on Fluoropak 80 (powdered Teflon from Analabs) to get a fraction that was largely TFEA-d_2 mixed with some other volatiles. Partly fluorinated TBrEA fractions were eluted later. The second stage was on a 5-m column with the same packing at 0 °C. Finally, the TFEA-d_2 was dried again by passing it through the P_2O_5 column. The identity of TFEA-d_2 was confirmed by ^{19}F NMR (complex multiplet at $\delta = -137.27$ ppm) and deuterium NMR (multiplet at $\delta = 5.61$ ppm).

TFEA-$^{13}C_2$ was prepared in a similar manner from acetylene-$^{13}C_2$ (CDN Isotopes, Canada. 99% ^{13}C) as the starting material. For the intermediate TBrEA-$^{13}C_2$ the proton ($\delta = 5.98$ ppm) and the proton-coupled ^{13}C ($\delta = 46.88$ ppm) NMR spectra were identical AA′XX′ multiplets.[15] The absolute values of the coupling constants were $J_{CH} = 180.4$ Hz, $J_{CH'} = 1.2$ Hz, $J_{CC'} = 40.7$ Hz, and $J_{HH'} = 2.8$ Hz. For the final product, TFEA-$^{13}C_2$, the proton spectrum ($\delta = 5.72$ ppm) is a complex multiplet with two prominent peaks split by 193.0 Hz. The ^{19}F spectrum ($\delta = -136.58$ ppm) is a complex multiplet with four prominent peaks split by 211.2 and 56.2 Hz. The proton-decoupled ^{13}C spectrum ($\delta = 109.21$ ppm) is a complex multiplet with a prominent triplet structure split by 211.2 Hz.

For normal TFEA, the natural abundance ^{13}C spectrum with proton decoupling has $\delta = 109.22$ ppm, $J_{CF(gem)} = 246.4$ Hz and $J_{CF(vic)} = 35.0$ Hz. For the complex proton and ^{19}F spectra the shifts are 5.72 ppm and −136.46 ppm. These latter two spectra have been fully analyzed before.[16]

Proton NMR spectra of the partly fluorinated TBrEA products are useful in identifying these new intermediates and following the course of the reaction. Proton-decoupled ^{13}C and proton-coupled ^{19}F spectra were also recorded but are not reported here. Also unreported are spectra of deuterium- and ^{13}C-substituted intermediates.

For 1,1,2-tribromo-2-fluoroethane, the multiplet centered at 5.79 ppm is for the CBr_2H end and is a doublet of doublets with $J_{HF(vic)} = 13.0$ Hz and $J_{HH} = 3.8$ Hz. The multiplet centered at 6.56 ppm is for the CBrFH end and is a doublet of doublets with $J_{HF(gem)} = 48.9$ Hz and $J_{HH} = 3.8$ Hz.

For 1,1-dibromo-2,2-difluoroethane, the multiplet centered at 5.57 ppm is for the CBr_2H end and is a triplet of doublets with $J_{HF(vic)} = 9.8$ Hz and $J_{HH} = 3.5$ Hz. The multiplet centered at 5.86 ppm is for the CF_2H end and is a triplet of doublets with $J_{HF(gem)} = 55.6$ Hz and $J_{HH} = 3.5$ Hz.

For 1-bromo-1,2,2-trifluoroethane, the multiplet centered at 5.89 ppm is for the CF_2H end and is a triplet of triplets (partly resolved splitting in the center triplet) with $J_{HF(gem)} = 54.5$ Hz, $J_{HF(vic)} \approx 4.0$ Hz and $J_{HH} = 4.0$ Hz. The multiplet centered at 6.35 ppm is for the CBrFH end and is a doublet of triplets of doublets with $J_{HF(gem)} = 48.4$ Hz, $J_{HF(vic)} = 6.8$ Hz and $J_{HH} = 4.0$ Hz.

Gas-phase infrared spectra can also be used to follow the progress of fluorination. The tribromomonofluoro intermediate is, however, too involatile to sample in this way. Distinguishing features in cm^{-1} are as follows. The spectrum of the dibromodifluoro species has Q branches at 2990 and 2972, medium intensity features at 1375, 1164, 744, and a very strong triplet at 1098. The spectrum of the trifluoromonobromo species has a Q branch at 3006, a very strong doublet at 1128, 1121, and a medium triplet at 763.

Spectroscopy. Midrange- and far-infrared spectra were recorded on Perkin-Elmer FT 1760 and 1700X spectrometers, respectively. Gas-phase samples were contained in stopcock-equipped, 10-cm Wilmad mini cells with 25-mm diameter cesium iodide or polyethylene windows. For low-temperature, crystal-phase samples, a Hornig-type cold cell with cesium iodide windows was used. A thin sample was sprayed onto the liquid nitrogen cooled interior window and then annealed by raising the temperature incrementally and checking for increased crystallinity in the spectrum recorded at 77 K. Typically, 25 scans at 0.5 cm^{-1} resolution were accumulated for midrange spectra, and 200 scans at 1.0 cm^{-1} resolution were recorded for the far-infrared spectra. For all spectra that included regions with water bands the instruments were purged with dry nitrogen.

Raman spectra were recorded with a Spex Ramalog 5 instrument and its associated Nicolet 1180 minicomputer. The 514.5-nm exciting line was produced by a Coherent Innova 70 argon-ion laser. Plasma lines were removed with a home-built Amici prism system or with a Kaiser Optical corner cube. Samples were contained in 1.8-mm capillaries and mounted in a Harney-Miller-type cold cell cooled by a regulated stream of cold nitrogen gas. The cell temperature was adjusted to −80 °C for liquid-phase samples and −105 °C for crystal-phase samples. The instrument has 90° sample geometry with a polarization filter in the scattered beam. For liquid-phase samples, both perpendicular and parallel positions of the filter were used, and four scans were accumulated for each setting. For crystal-phase samples, the polarization filter was removed, and a Kaiser Optical notch filter was used to remove the exciting line from the scattered light. All spectra were recorded with about 2.5 cm^{-1} resolution, and frequency accuracy is ±2 cm^{-1} based on calibration with an argon pencil lamp. Reported spectra were treated with a nine-point smoothing function.

NMR spectra were recorded in $CDCl_3$ solutions on a Bruker AC 200 instrument and referenced to external TMS or $CFCl_3$.

Results and Discussion

Selection Rules and General Remarks. The two rotamers of TFEA have different symmetries and therefore different selection rules. For the normal species as well as for both isotopomers, the anti rotamer has C_{2h} symmetry. The vibrational fundamentals comprise six a_g modes, four a_u modes, three b_g modes, and five b_u modes. Mutual exclusion applies to this centrosymmetric molecule, and only the a_u and b_u modes are infrared-active. The *a* and *c* principal rotation axes lie in the plane of symmetry with the *a* axis passing through the center of the CC bond and close to bisecting the line between the two fluorine atoms on each end. The *b* principal axis is perpendicular to the plane of symmetry and coincident with the 2-fold symmetry axis. Thus, in the gas-phase spectrum, the a_u modes are associated with B-type bands, and the b_u modes are associated with hybrid A/C-type bands. Only the a_g and b_g modes are Raman-active. The a_g modes give polarized bands, and the b_g modes give depolarized bands.

For the normal species as well as both isotopomers, the gauche rotamer has C_2 symmetry. Its fundamentals consist of 10 a modes and 8 b modes, all of which are both infrared- and Raman-active. The a modes give polarized bands, and the b modes give depolarized bands in the Raman spectrum. The symmetry axis is also the *c* principal rotation axis. Thus, modes of the a symmetry species have C-type shapes, and the modes of the b symmetry species have hybrid A/B-type shapes in the gas-phase infrared spectrum.

TABLE 1: Moments of Inertia for Three Isotopomers of the Anti Rotamer and for the Gauche Rotamer of TFEA (in amu Å²)

species	I_a	I_b	I_c
anti rotamer			
normal species[a]	98.338	160.378	245.068
$^{13}C_2$ species[b]	98.538	161.514	245.999
d_2 species[b]	102.333	165.092	245.782
gauche rotamer			
normal species[a]	96.191	178.076	198.832

[a] From ref 10. [b] Computed from geometric parameters in ref 10.

Table 1 gives the moments of inertia of the two rotamers of TFEA and of the two isotopic modifications of the anti rotamer. The moments of inertia of the normal species are observed values.[10] The moments of inertia of the $^{13}C_2$ and d_2 isotopomers were computed from the provisional geometric parameters reported by Stone et al.[10] The moments of inertia of the isotopomers of the anti rotamer are used in the product rule calculations reported below. Both rotamers are rather asymmetric tops with $\kappa = -0.295$ and -0.756 for the normal anti and gauche rotamers, respectively.

Kalasinsky and co-workers observed two different solid forms in the Raman spectrum of the normal species, forms I and II.[6] Although we did not repeat a study of the Raman spectrum of the normal form in the condensed phase, we saw no evidence of differences in the Raman spectra of the $^{13}C_2$ or d_2 species that could be attributed to two different solid forms. Of course, some differences occur that can be attributed to annealing.

A puzzling feature of the spectra of tetrafluoroethane is the decided increase in the CH stretching frequency in going from the gas phase to the crystal phase. This behavior is present but unremarked upon in the spectra of the normal species as reported before.[6] The up-frequency shifts in the infrared spectrum are 49, 45, and 5 cm^{-1} for the normal, $^{13}C_2$, and d_2 species, respectively. For the normal species in the Raman spectrum, the corresponding up-frequency shift is 31 cm^{-1}.[6] Such large, up-frequency shifts in going from the gas phase and the liquid phase to the crystal phase are unexpected. A possible, but questionable, explanation is hydrogen bonding. In going from the gas phase to the crystal phase, one expects stretching modes to decrease in frequency and bending modes to increase in frequency with hydrogen bonding.[17] In addition, although the shift due to hydrogen bonding should be smaller for CD bonds than for CH bonds, the difference observed for TFEA isotopomers is too large. The bending modes do increase in frequency some. These up-frequency shifts are 8, 7 cm^{-1} and 8, 8 cm^{-1} for the infrared-active modes of the normal and $^{13}C_2$ species, respectively. Small shifts downward occur, however, for the d_2 species. Another possibility for the unusual frequency shifts is a marked crystal splitting with the other component being inactive in each spectrum. Thus, only the upward frequency shift is apparent. Neither explanation is fully satisfactory.

In the discussion of assignments that follows, we consider first the assignments of the anti rotamers of all three isotopomers. These assignments are more secure and prepare the way for the gauche assignments. Because the lower-energy, anti form is the only rotamer present in the crystal phase, examina-

TABLE 2: Vibrational Fundamentals of the Anti Rotamers of TFEA and Its $^{13}C_2$ and d_2 Isotopomers (in cm^{-1})

selection rules and approximate descript.	normal species obs.[a]	normal species calc.[b]	$^{13}C_2$ species obs.	d_2 species obs.[c]
a_g: Raman-active, pol.				
ν_1 sym. C−H(D) stretch	3004 m	3202	2999 m, p	2231[d] m, p
ν_2 sym. C−H(D) bend	1443 w, dp	1532	1420[d] w, p?	914 m, p
ν_3 sym. CF_2 stretch	1145 m, p	1205	1131 m, p	1333 w, p?
ν_4 C−C stretch	1097 s, p	1148	1061 s, p	1062 s, p
ν_5 sym. CF_2 bend	623 vs, p	628	619 vs, p	608 vs, p
ν_6 sym. CF_2 rock	361 vs, p	363	361 s, p	362 s, p
a_u: IR-active, B-type				
ν_7 asym. C−H(D) flap	1331 s, B	1416 s	1325 s, B	956 m, B
ν_8 asym. CF_2 stretch	**1144.3** vs, B	1203 vs	1117 vs, B	1172.1 vs, B
ν_9 asym. CF_2 twist	210 w, B	203 w	209 w, B	210 w, B?
ν_{10} torsion	82 m?, B	91 w	82 w, B	82 w, B?
b_g: Raman-active, depol.				
ν_{11} asym.′ C−H(D) flap	1362 m, dp	1446	1355 m, dp	956 m, dp
ν_{12} asym.′ CF_2 stretch	1083 sh, dp	1171	1053[e] m	1159 w, dp
ν_{13} asym.′ CF_2 twist	479 m, dp	495	478 w, dp	472[e] w
b_u: IR-active, A/C-type				
ν_{14} sym.′ C−H(D) str.	2995 s, C	3212 s	2987 s, C	2218 s, C
ν_{15} sym.′ C−H(D) bend	**1309** s, C	1358 s	1299 s, C	1015 s, C
ν_{16} sym.′ CF_2 stretch	1127.4 vs, A/C	1166 vs	1101 vs, A/C	1129.5 vs, A/C
ν_{17} sym.′ CF_2 bend	542 m, A	535 m	539 s, A	539 m, A
ν_{18} sym.′ CF_2 rock	413[f] s, ?	418 s	405[f] s, ?	372[f] s, A/C

[a] Reference 6 and additional infrared spectroscopy. Here, as elsewhere in the table, frequencies are for the liquid phase in Raman spectra and the gas phase in infrared spectra. Abbreviations: vs, very strong; s, strong; m, medium; w, weak; vw, very weak; sh, shoulder; p, polarized; dp, depolarized; band shapes: A, A-type; B, B-type; C, C-type; A/C, hybrid. [b] Reference 7. Numerical values for calculated absorptivities are for a_u modes, 60, 337, 2, 2, respectively, and for b_u modes, 54, 37, 204, 10, 50, respectively. [c] CD-rich modes are listed according to the approximate description rather than in numerical order. [d] Fermi resonance multiplet. [e] Crystal-phase value. [f] Extensive structure.

tion of the crystal-phase infrared and Raman spectra gives direct evidence for bands due to the anti species. At room temperature, the gauche rotamer contributes only about 25% in the gas phase,[18] and many of its bands are close to those of the anti rotamer. The amount of the gauche rotamer increases to about 44% in the liquid phase at −80 °C due to its polarity. Thus, the contribution of the gauche rotamer is more apparent in the Raman spectrum for the liquid phase even at low temperature. Overall, the evidence for the assignments for the gauche rotamers is weaker than for the anti rotamers.

In the far-infrared spectra many lines due to residual water vapor in the spectrometer or from evaporation from the walls of the glass sample cell are present and should be overlooked in interpreting the band shapes.

Assignment for the Anti Rotamer of Normal TFEA. The assignment for the normal species of TFEA agrees for the most part with the work of Kalasinsky and co-workers.[6] Thus, we comment only on those assignments which are changed from the previous ones or which remain in doubt. Table 2 summarizes the fundamentals for the anti rotamers of TFEA and its two isotopomers.

We reexamined the gas-phase and crystal-phase infrared spectra of the normal species of TFEA except in the far-infrared region. In addition, we had available the high-resolution (0.002 cm^{-1}) infrared spectrum of the 900−1250-cm^{-1} region. This gas-phase infrared spectrum for the very intense CF_2 stretching region was recorded on a Bruker IFS 120HR instrument in a 3-m cell at −100 °C (pressure about 0.15 Torr) by Dr. Michael Lock at Justus Liebig University in Giessen, Germany. The full analysis of the rotational structure in this spectrum is the subject of a future paper, in which the spectrum will be shown. Because the infrared spectra of the $^{13}C_2$ species, which are part of the present report, are close to the spectra of the normal species and because the infrared spectra of the normal form have been reported before,[6] the infrared spectra of the normal species are not included in this paper.

In general, our infrared spectra agreed with the previous report.[6] The exceptions were that the crystal-phase spectrum showed a distinct medium-weak doublet near 1300 cm^{-1}, the medium-resolution gas-phase spectrum showed a small Q-branch feature in the midst of the overlap region of the B-type and C-type bands in the 1320 cm^{-1} region, and the high-resolution infrared spectrum gave definitive information about the CF_2 stretching region. At the low temperature of the high-resolution infrared experiment, the gauche rotamer makes a small contribution of about 12% to the gas-phase mixture. From the high-resolution spectrum it is certain that two intense bands due to the anti rotamer overlap to give added strength to the central feature. Furthermore, the higher frequency band centered at 1144.34 cm^{-1} is of B-type shape, and the lower frequency band centered at 1127.43 cm^{-1} is of A/C-type shape with the A-component dominant. A definite Q branch is present in the 1127-cm^{-1} band in the spectrum at −100 °C. In addition, Stone et al. investigated the lower frequency band with a diode-laser, cold-jet-expansion technique and observed the stronger A-type and weaker C-type character.[10] In the previous report, the B-type center at 1144 cm^{-1} in the low-resolution infrared spectrum was assigned to the gauche rotamer, the strong central feature at 1136 cm^{-1} was assigned to ν_8 of the anti species, and the feature at 1125 cm^{-1} was assigned to the ν_{16} of the anti rotamer.[6] The B-type band is now confidently assigned to ν_8 of the anti species, and the A/C-type band remains assigned to ν_{16} of the anti species but with an adjustment in frequency to the band center.

A second revision in the assignment for the anti rotamer of the normal form is in the interpretation of the CH bending region of the infrared spectrum. Kalasinsky and co-workers chose the common central branch of the B-type and C-type bands for ν_{15} for the anti rotamer. We consider the strong Q branch of the C-type band at 1309 cm^{-1}, which they assigned to the gauche rotamer, to be a better choice for the anti rotamer. This band correlates well with a medium-weak doublet, which is regarded as crystal splitting, in the infrared spectrum of the crystal phase.

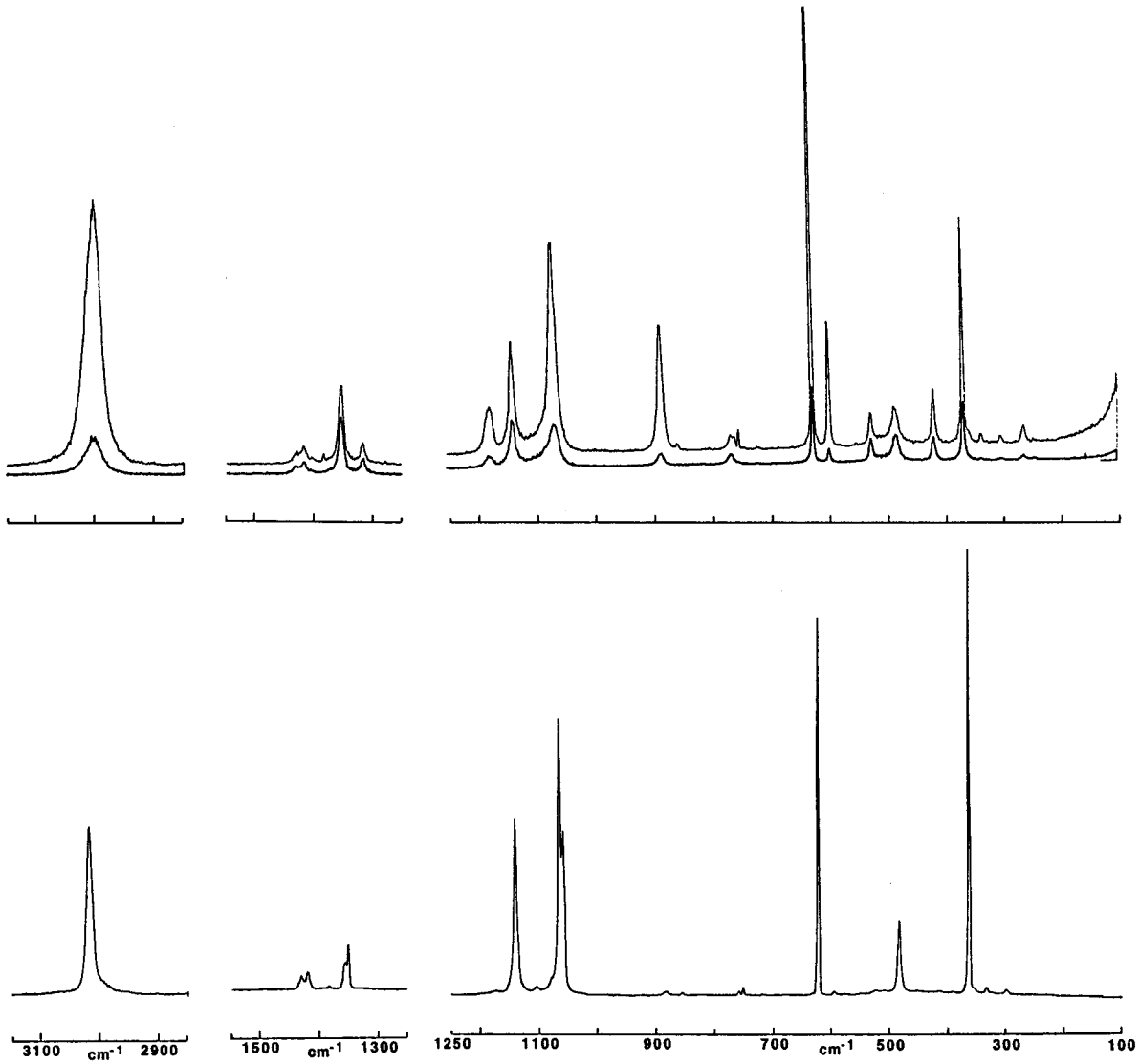

Figure 1. Raman spectra of 1,1,2,2-tetrafluoroethane-$^{13}C_2$. Upper trace, liquid at −80 °C with parallel and perpendicular settings of the polarization analyzer; lower trace, crystal-phase spectrum at −105 °C.

No binary combination tone of B_u symmetry for the anti rotamer is predicted near this frequency, which could otherwise explain the doublet.

One other issue relates to the assignment of the infrared-active fundamentals for the anti rotamer of the normal form. This issue is the strength of the evidence for $\nu_{10}(a_u)$. Kalasinsky et al. assigned the band of B-type shape in the gas-phase infrared spectrum at 82 cm^{-1} to the ν_{10} fundamental. They did not, however, investigate the spectrum of the crystal phase in this region. Thus, this band could be due to the gauche rotamer. However, not only is the anti rotamer three times more abundant in the gas phase, but the recent calculations of infrared intensities by Kenny and co-workers,[7] described more fully below, predict a very weak intensity for the corresponding band for the gauche rotamer compared to a weak intensity for this band of the anti rotamer. Thus, it seems certain that the observed band is due to the anti rotamer.

In the gas-phase infrared spectrum of TFEA, Kalasinsky et al. observed extensive structure going to higher frequency associated with the band at about 413 cm^{-1}. They assign this structure to hot bands involving various levels of excitation of the torsion, $\nu_{10}(a_u)$, interacting with ν_{18}. We offer a different interpretation below in the section on TFEA-d_2.

The evidence for the Raman-active modes comes entirely from the work of Kalasinsky et al., who examined the Raman spectrum in the gas phase as well as in the liquid and crystal phases. For only one Raman-active mode is the spectral evidence questionable. That mode is ν_{12} of the b_g symmetry species. The evidence for this fundamental is a shoulder in the spectra of gas and liquid phases which becomes a distinct feature in the crystal-phase spectrum at 1080 cm^{-1}. A similar feature is seen in the crystal-phase Raman spectrum of the $^{13}C_2$ isotopomer. Strong evidence for this assignment comes, moreover, from the spectra of the d_2 isotopomer, as discussed below.

In summary, the assignment of the eighteen vibrational fundamentals of the anti rotamer of the normal species is, with the possible exception of ν_{12}, now on a firm experimental footing. In Table 2 the experimental evidence for these assignments is given, and the frequencies are compared with those computed by Kenny et al. with an MP2/6-31G** model without scaling.[7] With the exception of two low frequencies and the strongly anharmonic CH stretching frequencies, the experimental frequencies are lower with an average difference of −39 cm^{-1}. The largest difference is −89 cm^{-1} for the CH bending mode at 1443 cm^{-1}. The questionable assignment of the ν_{12} mode differs from the calculated value by −88 cm^{-1}.

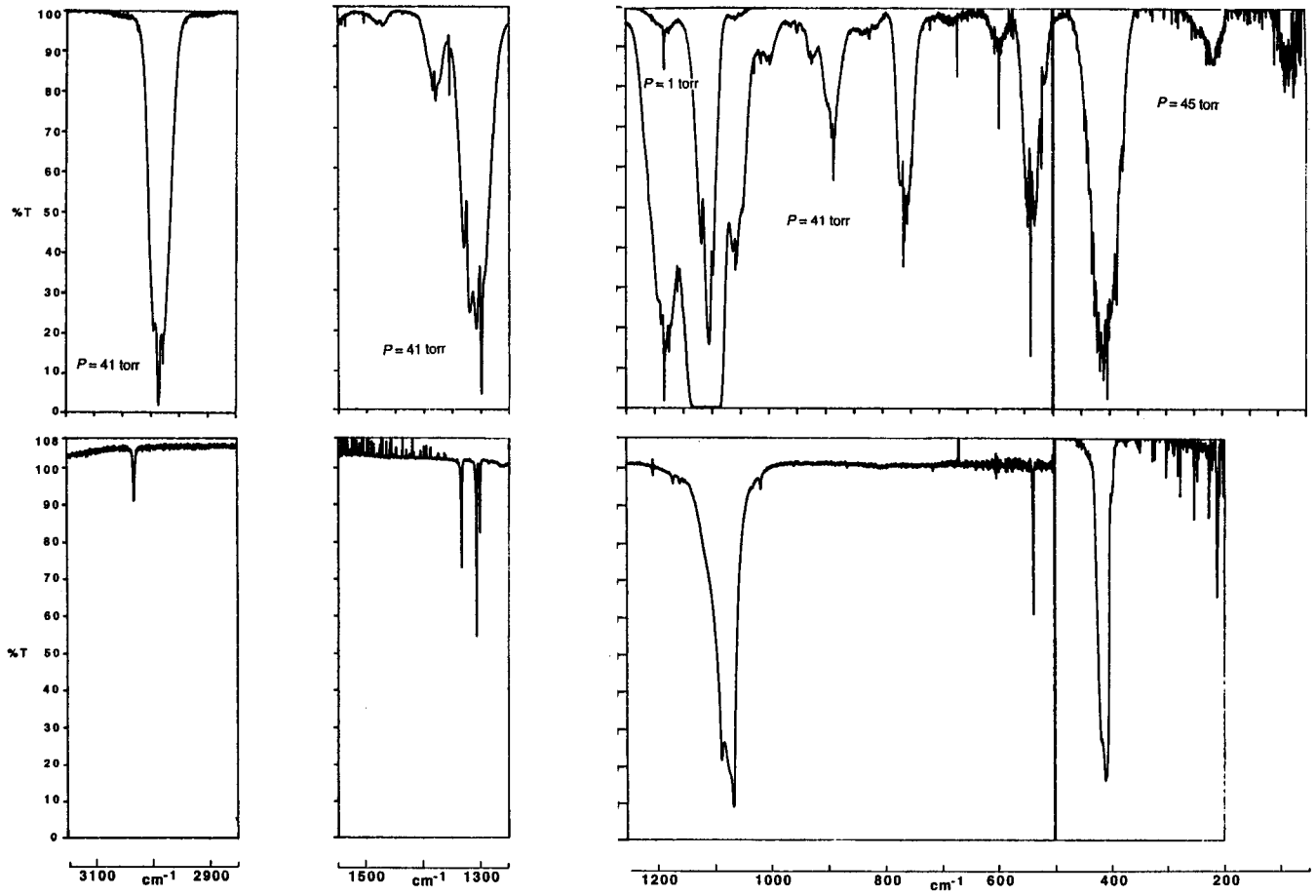

Figure 2. Infrared spectra of 1,1,2,2-tetrafluoroethane-$^{13}C_2$. Upper trace, gas phase; lower trace, crystal phase at −196 °C after annealing at higher temperatures.

In addition, as seen in Table 2, the calculated intensities for infrared transitions agree qualitatively with the observed ones. Overall, the comparison with the calculated frequencies supports the assignment made from experimental data. Assignments which differ from the work of Kalasinsky and co-workers are in boldface in Table 2. The increased accuracy for ν_8 and ν_{16} is based on an analysis of the rotational structure in the high-resolution infrared spectrum. In supplementary Table S1, all of the features in the infrared and Raman spectra, including the weak ones due to combination tones, are assigned.

Assignment for the Anti Rotamer of TFEA-$^{13}C_2$. In general, the assignment of fundamentals for the anti rotamer of the $^{13}C_2$ isotopomer proceeds directly from the assignments for the anti rotamer of the normal species. Of course, decreases in frequency are expected for the substitution of heavier isotopic masses, although these shifts will be relatively small for ^{13}C substitution. Frequencies that depend strongly on motions of the CH bonds will change little, whereas frequencies that depend on heavy atom motions will change more.

Figure 1 gives the Raman spectra of TFEA-$^{13}C_2$ in the liquid and crystal phases. From the crystal-phase Raman spectra clear evidence exists for all of the a_g and b_g fundamentals except two. A weak doublet is found near 1420 cm^{-1}. This doublet must be due to ν_2, which also has a weak band in the Raman spectrum of the normal species. The doublet can be explained as Fermi resonance with $\nu_4 + \nu_6$ (A_g), which is predicted at 1422 cm^{-1}. The most uncertain assignment is for ν_{12}, which was also uncertain for the normal species. Only eight distinct bands are seen for nine Raman-active modes in the crystal-phase spectrum. A shoulder is found, however, at 1053 cm^{-1} in the crystal-phase spectrum in Figure 1. We adopt this feature for ν_{12} in accord with the corresponding assignment for the normal species. Depolarization information gives further support to the distinction between a_g and b_g modes. Table 2 gives details of the spectroscopic features of bands assigned to the a_g and b_g fundamentals in comparison with those for the normal species.

Figure 2 gives the infrared spectra of TFEA-$^{13}C_2$ in the gas and crystal phases. The high-resolution gas-phase spectrum has been recorded from 880 to 1200 cm^{-1} at −100 °C at Giessen, but the rotational structure is yet to be analyzed. The crystal-phase spectrum contains good evidence for eight of the nine infrared-active fundamentals when each of the two features in the very intense CF_2 stretching region between 1000 and 1100 cm^{-1} is taken to represent a fundamental. Evidence for the ninth infrared-active fundamental is found in the gas-phase spectrum at 82 cm^{-1} below the accessible range of the low-temperature cell used for crystal-phase spectra. This assignment of ν_{10} is confidently made on the same basis as was used for the equivalent mode in the normal species. Band shapes, including those now available from the high-resolution spectrum of the $^{13}C_2$ species in the CF stretching region of the gas-phase spectrum, provide further support to the assignments.

A striking difference between the infrared spectra of the $^{13}C_2$ species and the normal species is the two-times greater intensity of the bands due to CF_2 stretching in the spectrum of the $^{13}C_2$ species. Because the intensity of the bands due to CH bending are comparably weaker in the spectrum of the $^{13}C_2$ species, the mixing of CF_2 stretching with the bending modes must be greater in the normal species. This diminished transfer of intensity from the CF_2 stretching modes to the CH bending

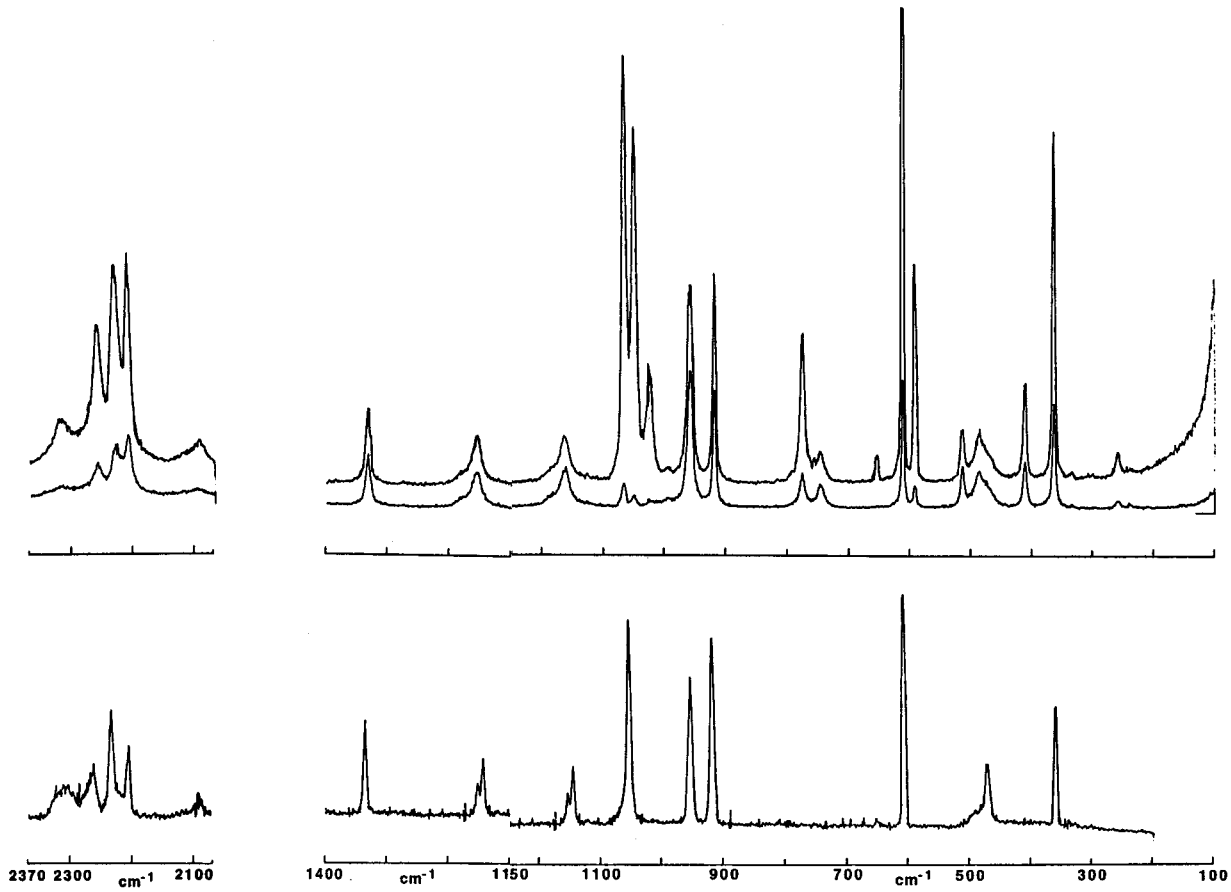

Figure 3. Raman spectra of 1,1,2,2-tetrafluoroethane-d_2. Upper trace, liquid at −80 °C with parallel and perpendicular settings of the polarization analyzer; lower trace, crystal-phase spectrum at −105 °C.

TABLE 3: Teller−Redlich Product Ratios for the Anti Rotamer of TFEA

molecules	sym. species	obs. ratio	calc. ratio	difference
$^{13}C_2$/normal	a_g	0.932	0.926	0.6%
	a_u	0.967	0.970	0.3%
	b_g	0.965	0.965	0.2%
	b_u	0.943	0.941	0.2%
d_2/normal	a_g	0.519	0.508	2.2%
	a_u	0.736	0.714	3.1%
	b_g	0.740	0.723	2.3%
	b_u	0.516	0.510	1.2%

modes in the spectrum of the $^{13}C_2$ species is consistent with the greater frequency difference between the two types of modes for the $^{13}C_2$ species. The greater frequency difference is a consequence of the greater ^{13}C isotope effect on the CF_2 modes than on the CH bending modes.

The assignments of all eighteen fundamentals of TFEA-$^{13}C_2$ are given in Table 2 in comparison with those of the normal species. Except for ν_{10}, which appears unchanged, all fundamentals of the $^{13}C_2$ species have lower frequencies than their counterparts for the normal species. Thus, the Rayleigh Rule for isotopic substitution is satisfied. In addition, the frequency shifts are largest for modes in the central part of the infrared region for which substitution of ^{13}C is expected to have the largest effect on normal modes. A quantitative check on the assignment for the $^{13}C_2$ species in relation to the assignment for the normal species is provided by the Teller−Redlich product rules. The satisfactory comparison of the observed frequency product ratios for each symmetry species with the predicted ones is shown in Table 3. Supplementary Table S2 gives the details of the spectra of the $^{13}C_2$ species and their assignments.

Assignment for the Anti Rotamer of TFEA-d_2. Figure 3 contains the Raman spectra of TFEA-d_2 in the liquid and crystal phases. In the Raman spectrum of the crystal phase, nine bands with some complications due to crystal splitting and Fermi resonance are found for the anti rotamer. Reinforced with polarization data from the liquid-phase Raman spectrum, the assignment of the nine Raman-active fundamentals of the anti rotamer is straightforward. Selection of the correct frequency for ν_{13} of b_g symmetry is, however, a problem. The obvious peak in the liquid-phase Raman spectrum in the 480-cm^{-1} region gives a frequency that is larger than the value for the normal isotopomer. The corresponding peak in the crystal-phase spectrum is at 472 cm^{-1}, which is a reasonable value. We use this frequency in Table 2. The change in intensity pattern between the liquid phase and the crystal phase either reflects the loss of an overlapping band due to the gauche rotamer or Fermi resonance. A combination tone for the gauche rotamer is predicted as $\nu_8 + \nu_{10} = 483$ cm^{-1} (A) but is unlikely to have sufficient intensity. A possible partner for Fermi resonance in the anti rotamer is $\nu_{10} + \nu_{18}$ (B_g), which has a predicted gas-phase frequency of 454 cm^{-1}. If the frequencies of the contributing fundamentals increase between the gas phase and the liquid phase, as is observed for some low-frequency modes, then Fermi resonance is possible. We favor this latter explanation. Strong spectral evidence for ν_{12}, which was a doubtful assignment for the other two isotopomers, is the depolarized band at 1159 cm^{-1} in the Raman spectrum. All the frequencies of the Raman-active fundamentals and their spectral evidence are summarized in Table 2 in comparison with the assignments for the normal and $^{13}C_2$ isotopomers.

Figure 4 contains the infrared spectra of TFEA-d_2 in the gas

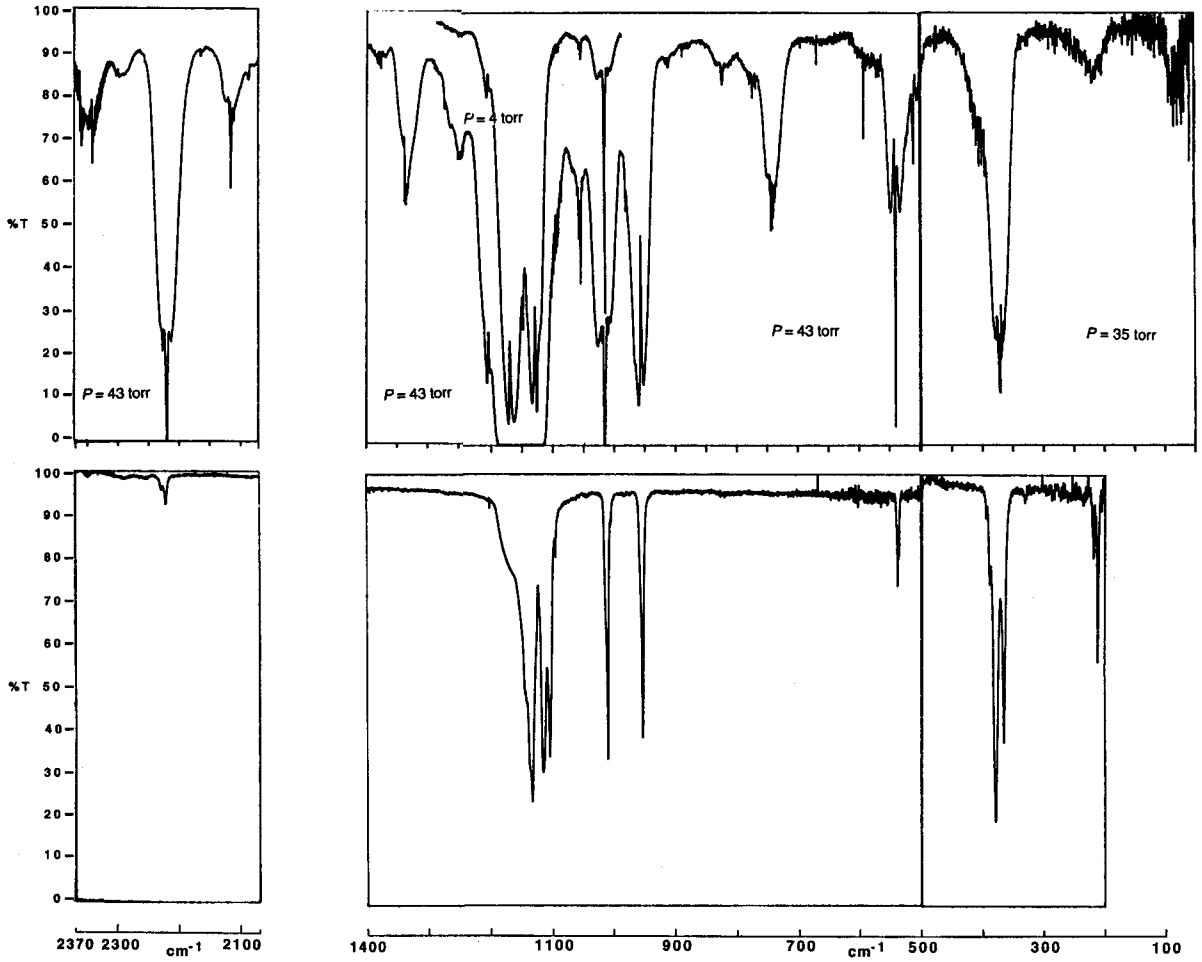

Figure 4. Infrared spectra of 1,1,2,2-tetrafluoroethane-d_2. Upper trace, gas phase; lower trace, crystal phase at −196 °C before annealing.

and crystal phases. The high-resolution infrared spectrum in the gas phase was recorded from 930 to 1230 cm^{-1} at −100 °C in Giessen. With an allowance for crystal splitting, eight bands for the anti rotamer are evident in the crystal-phase spectrum. The remaining fundamental is the band at 82 cm^{-1} of probably B-type shape in the gas-phase infrared spectrum. Elsewhere in the gas-phase infrared spectrum, band shapes support the assignments to the a_u and b_u symmetry species. Reasonable frequency shifts are found for modes that are rich in CD motion. Notable changes are observed in the two antisymmetric CF_2 stretching frequencies compared to the spectrum of the normal species. These bands have higher frequencies than for the normal species. This adjustment is consistent with the Rayleigh Rule because the frequencies of CD bending modes are below those of the CF_2 stretching modes, whereas the frequencies of CH bending modes are above. In the summary of frequencies of fundamentals of the d_2 species in Table 2, the CD-rich bending modes are aligned with the approximate descriptions and not in the conventional frequency order. As given in Table 3, the application of the Teller−Redlich rule shows that the assignments of the fundamentals for the normal isotopomer are consistent with those of the d_2 isotopomer.

As noted in the discussion of the spectrum of the normal species, unusual and extensive structure extends to the high-frequency side of the band for $\nu_{18}(b_u)$ near 418 cm^{-1} in the infrared spectrum. For the d_2 species this structure is less pronounced and further from the band center for ν_{18}. In addition, the band shape for ν_{18} of the d_2 isotopomer is less distorted. For the normal species, Kalasinsky and co-workers assigned this structure to hot bands of the type $\nu_{18} + n\nu_{10} - n\nu_{10}$.[6] That these features are so prominent, widely spaced by about 4 cm^{-1}, of comparable intensity, and on the high-frequency side of the band raises doubt about this interpretation. The significant displacement of these features to the high-frequency side of the ν_{18} band in the spectrum of the d_2 species is strong evidence against the simple hot band interpretation. A more satisfactory interpretation attributes these features to Coriolis coupling between the upper state of the ν_{18} transition and the series of upper states for the transitions $\nu_6 + (n + 1)\nu_{10} - n\nu_{10}$. For n of 1, $\nu_6 + \nu_{10}$ (A_u) is within one cm^{-1} of 444 cm^{-1} for all three isotopomers. Coriolis coupling is allowed because the symmetry product $A_u \times B_u$ is B_g, which is the symmetry species of two rotations. Frequencies of the three series of sharp lines are in footnotes to Tables S1, S2, and S3.

All of the assignments of fundamentals of the anti rotamer of the d_2 isotopomer are firmly based on experimental evidence. Since these assignments are consistent with those for the normal species as reflected in the satisfactory product rule ratios in Table 3, we have strong evidence in support of the one doubtful assignment for the normal species, namely, for ν_{12}. In turn, the corresponding assignment of ν_{12} for the $^{13}C_2$ species is supported. The increased accuracy in the values for ν_8 and ν_{16} comes from the analysis of the rotational structure in the high-resolution infrared spectrum. Supplementary Table S3 gives all of the observed bands for the d_2 species, including the weaker ones, and their assignments.

Probable Impurity. A series of seven sharp, weak features begins at 1089.1 cm^{-1} and runs to 1101.7 cm^{-1} in the infrared spectrum of the gas phase, Figure 4, of TFEA-d_2. These lines are spaced almost equally by about 2 cm^{-1}. Since these features

TABLE 4: Vibrational Fundamentals of the Gauche Rotamers of TFEA and its $^{13}C_2$ and d_2 Isotopomers (in cm^{-1})

selection rules and approximate descript.	normal species			$^{13}C_2$ species		d_2 species[c]	
	Raman[a]	IR[a]	calc.[b]	Raman	IR	Raman	IR
a: Raman, pol.; IR, C-type							
ν_1 sym. C−H(D) stretch	3004 p		3197 m	2999 m,p		2231 m,p	
ν_2 sym. C−H(D) bend		**1432** w, C	1510 w				
ν_3 sym. C−H(D) rock		**1363** mw, Q	1451 m		1355 w, C	772 m, p	773 w, ?
ν_4 sym. CF_2 stretch	1195 m, p	1206 m, C	1249 s	1168 m, p	1183 s, C		1338 m, C
ν_5 sym.′ CF_2 stretch	**1100** sh	[1105]	1165 w			1046 s, p	1053 m, C
ν_6 C−C stretch	898 m, p	905.8 m, C	953 m	879 m, p	885 m, C		
ν_7 sym. CF_2 flap	595 m, p	598 w, C	601 w	591 m, p	595 m, C	588 m, p	591 w, C
ν_8 sym. CF_2 deform.	412 m, p		413 w	412 w, p		408 m, p	
ν_9 sym. CF_2 twist	257 w, p		253 w	259 w, p		258 w, p	
ν_{10} torsion		[75]	83 vw				
b: Raman, depol.; IR, A/B type							
ν_{11} asym. C−H(D) stretch		3003 m, Q	3189 m		2979 m, Q		2225 w, A?
ν_{12} asym. C−H(D) bend	1390[d] sh	1393 w, B	1477 m		1382 w, B		
ν_{13} asym. C−H(D) rock	1323 w, dp	**1320** m, Q	1392 m	1318 w, dp		991 vw, dp	
ν_{14} asym. CF_2 stretch		[1135]	1194 vs				1204 m, B?
ν_{15} sym.′ CF_2 stretch		1075 w, ?	1161 m		1047 w, sh		
ν_{16} asym. CF_2 flap	775 w, dp	780 ms, A	803 s	760 w, dp	763 m, A	741 w, dp	743 m, ?
ν_{17} asym′ CF_2 deform.	530 vw, br	523 w, A	512 w	519 w, dp	520 sh, A	511 w, dp	510 w, A
ν_{18} asym. CF_2 twist	**247** w, p?	∼**240** w	232 w		∼240 w	240 vw, dp	∼240 w, ?

[a] See Table 2. Also, br, broad. [b] Reference 7. Numerical values of calculated absorptivities are for a modes, 47, 5, 25, 125, 9, 47, 5, 3, 2, 1, respectively, and for b modes, 23, 38, 36, 274, 36, 74, 15, 6, respectively. [c] See Table 2. [d] Gas-phase value.

appeared with equal intensity in two different preparations of TFEA-d_2, we thought initially that these lines were due to difference tones involving $\nu_{12}(b_g)$ and transitions between various states in the $\nu_{10}(a_u)$ manifold. However, the intensities of the lines did not fall off as expected for difference tones, and these lines are present in the spectrum at −100 °C without an appreciable intensity falloff and with a width that is too narrow for Q branches of bands. In addition, similar series are not found for the sum tones at higher frequency in the infrared spectrum of TFEA-d_2. Nor are comparable lines for possible difference tones found in the spectra of the other two isotopomers. Thus, we conclude that this series of lines is due to an unidentified impurity with a relatively low molecular mass.

Assignment for the Gauche Rotamer of TFEA. Several adjustments in the previous assignment for the gauche rotamer of the normal species of TFEA are proposed.[6] Table 4 gives details of the assignments. Columns 1 and 2 of the data give the Raman and infrared spectral evidence, respectively, which is drawn from the work of Kalasinsky and co-workers and from our reexamination of the gas-phase and crystal-phase infrared spectra. Assignments that we have revised are shown in boldface type. Column 3 gives the predictions of frequencies and infrared intensities from the recent calculations of Kenny et al.[7]

For the modes of the a symmetry species, the previous choice of the C-type band in the infrared spectrum at 1362 cm^{-1} for ν_2 was made unreasonable by the calculated frequency of 1510 cm^{-1}. We have reassigned 1362 cm^{-1}, as 1363 cm^{-1}, to ν_3 of the gauche rotamer and have reassigned 1309 cm^{-1}, which had been assigned to ν_3, to the anti rotamer as discussed above. For ν_2 the only reasonable possibility is a weak, C-type band at 1432 cm^{-1} with an absorbance of about one-fifth of that of the C-type band at 1363 cm^{-1}. In accord with this observation, the calculations of Kenny et al. predict an absorbance ratio of five for these two bands. This predicted absorbance ratio also implies that the band for ν_2 should be observable. The alternative possibilities, the very weak Q branches at 1457 and 1413 cm^{-1}, are too weak to be credible assignments for ν_2. The band at 1432 cm^{-1} has extensive structure in the Q branch (about 1-cm^{-1} spacing) and fainter structure in the R branch (about 1.3-cm^{-1} spacing). This structure suggested that the band might be due to an impurity. None of the likely impurities that would have discernible rotational structure, CF_2H_2, CF_3H, or H_2FCCFH_2, accounts for the band. Support for accepting this structured band for ν_2 is the occurrence of extensive hot band structure associated with Q branches elsewhere in the spectrum. A combination tone predicted at 1429 cm^{-1} for $\nu_6 + \nu_{17}$ (B) is an alternative assignment for the 1432-cm^{-1} feature. This prediction is, however, based on gas-phase values and thus implies a yet lower frequency than 1429 cm^{-1} for the combination tone. Thus, we tentatively assign ν_2 as 1432 cm^{-1}. The C-type band at 1206 cm^{-1}, assigned to ν_4, decreases significantly in relative intensity in the infrared spectrum at −100 °C, thereby confirming this assignment to the gauche rotamer.

Another adjustment in the assignment for the a symmetry species of the gauche rotamer is to reject 1146 cm^{-1} for ν_5, which is predicted to have only a weak intensity in the infrared spectrum. This feature is now known to be the R branch of a B-type band of the anti rotamer based on the high-resolution infrared spectrum. In addition, because the CF_2 stretching frequencies for the anti rotamer are, on the average, 60 cm^{-1} below the calculated values, the calculated value of 1165 cm^{-1} suggests that this mode will be around 1105 cm^{-1}. With the band's weak predicted intensity and the low concentration of the gauche rotamer, this band is probably hidden under the very intense CF_2 stretching bands of the anti rotamer in the infrared spectrum. Another possibility is to interpret the shoulder, reported at 1100 cm^{-1} in the liquid-phase Raman spectrum and previously assigned as ν_{14}, as evidence for this totally symmetric fundamental. We have done so. Stone et al. investigated ν_6 with the jet-beam, high-resolution method.[10] From their analysis of the rotational structure, they made a definitive assignment as a C-type band with a band center of 905.834 cm^{-1}. This band for the gauche rotamer was observable at low temperature because vibrational relaxation from the gauche to the anti rotamer does not occur fully in the rapid cooling of the jet beam.

Three low-frequency modes of the a symmetry species remain to be discussed. For ν_8, which is strongly supported by a polarized Raman feature of medium intensity at 412 cm^{-1}, Kalasinsky et al. also assigned this mode to a Q-branch feature at 408 cm^{-1} in the infrared spectrum. Given the prediction of a weak intensity for the infrared transition for ν_8 and its near coincidence with the intense and complex band for ν_{18} for the

anti rotamer, we think it unlikely that the feature of medium intensity is due to ν_8 of the gauche rotamer. Similar reasoning rules out observing a band for ν_9 in the infrared spectrum, although this mode is represented by a polarized band at 257 cm^{-1} in the Raman spectrum. A weak intensity is predicted for the band for ν_9 in the infrared spectrum, and the greater intensity predicted for the band for ν_{18} should dominate this region. At present no direct spectral evidence exists for ν_{10}, which is calculated at 83 cm^{-1}. The infrared spectrum in this region is dominated by the band for the corresponding mode of the anti rotamer. A revised prediction of 75 cm^{-1} is based on the difference between the calculated and observed frequencies for the torsional mode of the anti rotamer. This prediction is consistent with the previous estimate of 72 cm^{-1}.[6] This estimate was made from the hot band structure of the infrared band at 780 cm^{-1} and a series of Q branches observed near 849 cm^{-1} at high sample pressure. We confirmed this latter observation.

For the modes of the b symmetry species, several comments apply. As discussed in the section on the anti rotamer of TFEA, we have revised the assignments in the CH bending region. We consider the small Q branch at 1320 cm^{-1} on top of the strong absorption caused by the overlap of two bands of the anti rotamer to be due to ν_{13} of the gauche rotamer. This choice is reinforced by the earlier designation of a depolarized Raman band of medium intensity at 1323 cm^{-1} for this mode. Unfortunately, the value of 1312 cm^{-1} from the gas-phase Raman spectrum does not agree with the value of 1320 cm^{-1} from the gas-phase infrared spectrum.[6] This discrepancy is discounted because the Raman band is reported as very weak and is not even apparent in the published spectrum.

The previous assignment of the ν_{14} to the shoulder at 1100 cm^{-1} in the Raman spectrum is unlikely because of a higher predicted frequency. As discussed above, this shoulder has been reassigned to a mode of the a symmetry species. An estimate for ν_{14} is about 1135 cm^{-1} (ca 1194−60 cm^{-1}). Despite the prediction of a very strong band in the infrared spectrum, the predicted frequency for the gauche rotamer falls in the region where the band would be overlapped by the intense CF_2 stretching modes of the more abundant anti rotamer. The estimate of 1135 cm^{-1} for ν_{14} in the gas phase is used in Table 4.

Evidence for ν_{15} is uncertain. The weak band of indistinguishable shape at 1075 cm^{-1} in the infrared spectrum was previously assigned to ν_{15}. Because this band appears to be absent from the spectrum at −100 °C, its assignment to the gauche rotamer is supported. Furthermore, no binary combination tone for the gauche rotamer is predicted near 1075 cm^{-1}. A drawback to this assignment is the estimated frequency of 1100 cm^{-1} (1161−60 cm^{-1}), which is 25 cm^{-1} above the observation.

The biggest adjustment in the assignments for the modes of the b symmetry species is replacing 495 cm^{-1} for ν_{18} with the approximate value of 240 cm^{-1}. The calculated frequency is 232 cm^{-1}. The predictions for all of the low-frequency modes of the anti rotamer are within 15 cm^{-1} of the observed values, and a similar agreement is seen for the gauche fundamentals that have been confidently assigned. The band for ν_{18} is probably contributing to the distinct hump on the high-frequency side of the distorted B-type band at 210 cm^{-1}. It is also possible that the weak liquid-phase Raman feature reported by Kalasinsky et al. at 247 cm^{-1} reflects this mode. This feature and its weak neighbor at 257 cm^{-1} are, however, both reported as polarized. No reasonable explanation exists for two polarized bands in this region. The weakness of the band may have contributed to uncertain polarization information.

In summary, the assignment of fundamentals for the gauche rotamer has been substantially revised but remains incomplete in contrast to the complete assignment for the anti rotamer. Table 4 summarizes the assignments. Experimental support for two of the CF_2 stretching modes, ν_5 and ν_{15}, is sketchy. No direct spectral evidence exists for one of the other CF_2 stretching modes, ν_{14}, or for the torsional mode, ν_{10}. The assignment for ν_{18} is guided by the calculated value, although some spectral evidence is available. Even though bands due to all of the fundamentals of the gauche rotamer are both infrared- and Raman-active, bands due to eight modes are observed in only one of the two spectroscopies. Overall the agreement between observed frequencies and calculated ones is comparable to that for the anti rotamer. Insofar as intensities can be compared, observations and calculations concur. Details of the assignment of all of the features of the spectra of TFEA are in supplementary Table S1.

Assignment for the Gauche Rotamer of TFEA-$^{13}C_2$. The assignment of vibrational fundamentals for the gauche rotamer of TFEA-$^{13}C_2$ follows directly from the assignment for the gauche rotamer of the normal species. The assignments from the Raman and infrared spectra are given in Table 4 in data columns 4 and 5, respectively. Figure 1 shows the liquid-phase and crystal-phase Raman spectra of TFEA-$^{13}C_2$. Figure 2 shows the gas-phase and crystal-phase infrared spectra of the $^{13}C_2$ species.

For the modes of the a symmetry species for the gauche rotamer of the $^{13}C_2$ species, only a few comments are needed. A weak feature for ν_2 is not found in the 1420-cm^{-1} region, as would be expected from the corresponding assignment of the normal species. However, as discussed above, weaker intensities are found for CH bending modes of the $^{13}C_2$ species in comparison with those of the normal species. In the high-resolution infrared spectrum the intensity of the C-type band at 1183 cm^{-1} decreases appreciably in going to −100 °C, thereby confirming that this band is due to the gauche rotamer. Frequency shifts between the two isotopomers are reasonable except that the frequency for ν_9 appears to shift up by 2 cm^{-1} in going to the heavier isotopomer. This apparent anomaly is attributed to uncertainties of ±2 cm^{-1} in measurements in the Raman spectra.

For the modes of the b symmetry species, a similar agreement is found between the observations for the $^{13}C_2$ species and the normal species. The pattern of Raman and infrared data is familiar with one exception. No Q branch appears for ν_{13} in the infrared spectrum, although a weak polarized band in the Raman spectrum at 1318 cm^{-1} reveals ν_{13}. As was the case for the normal species, no spectral feature is available for ν_{14}. The evidence for ν_{15} is more problematic than even for the normal species. In the infrared spectrum the feature at 1058 cm^{-1} persists at −100 °C and thus must be due to the anti rotamer. A weak broadening on the P-branch side of this band in the room-temperature spectrum appears to be absent at −100 °C. This feature is assigned to ν_{15} in accord with the interpretation for the normal species.

For ν_{18}, the evidence is the broad shoulder in the infrared spectrum in the 240 cm^{-1} region. This observation not only supports the assignment for the $^{13}C_2$ species but also reinforces the interpretation of the spectrum of the normal species. In assessing a weak feature of this type, it is regrettable that calculated Raman intensities are not available. All of the observed modes of the $^{13}C_2$ species for the b symmetry species

satisfy the Rayleigh Rule. In addition, shifts in frequencies due to substitution of the heavier isotope are reasonable.

In summary, the assignment of the vibrational fundamentals for the gauche rotamer of the $^{13}C_2$ species has a few more gaps than the incomplete assignment for the gauche rotamer of the normal species. Evidence for two CF_2 stretching modes is absent. No experimental evidence exists for the frequency of the torsion. Qualitatively, frequency shifts between the two isotopomers are reasonable. Satisfying these relationships reinforces the assignments for both species. Because of the gaps in the assignments, the Teller−Redlich product rule is inapplicable in assessing the assignments of the gauche rotamers of the d_0 and $^{13}C_2$ species. Details of the assignment of all of the features of the spectra of the $^{13}C_2$ species are in supplementary Table S2.

Assignment for the Gauche Rotamer of TFEA-*d*$_2$. Spectral data for use in the assignment of fundamentals of the gauche rotamer of TFEA-d_2 are in Figures 3 and 4. The first contains the Raman spectra; the second the infrared spectra. The assignments are summarized in Table 4, where data columns 6 and 7 are for the d_2 species. The numbering of frequencies for the d_2 species in Table 4 conserves approximate descriptions of normal modes rather than descending frequency order. Compared to the assignment for the gauche rotamer of the normal species, the assignment for the d_2 species is more problematic. A cause is the congestion of frequencies for CD bending modes with those for the CF and CC stretching modes.

Reasonable spectral evidence, mostly as polarized bands in the Raman spectrum, exists for six of the 10 fundamentals of the a symmetry species. In addition, an indistinct Q-branch feature at 2225 cm^{-1} is used for ν_{11} in accord with assignments for the gauche rotamers of the other two isotopomers. No spectral evidence exists for ν_2, which was a weak feature in the spectrum of the normal species, and no evidence exists for ν_6. The use of the strong Raman band at 1046 cm^{-1} for ν_5 is questionable. This band seems too intense for the minority component of the rotamer mixture. Attempts to attribute this band to Fermi resonance in the anti rotamer required an unlikely ternary combination. In addition, the crystal-phase spectrum shows no sign of splitting due to Fermi resonance. Supporting this assignment is a corresponding band at 1053 cm^{-1} in the infrared spectrum, which disappears at −100 °C. No evidence was found in the liquid-phase Raman spectrum for ν_{10}, the elusive torsional mode, despite searching down to the exciting line with a notch filter in front of the spectrometer slit.

For the modes of the b symmetry species, the spectral evidence is comparably scanty to that for the totally symmetric species. Features, albeit some questionable ones, exist for six of the eight fundamentals of this symmetry species. Good evidence exists for two CF_2 bending modes, ν_{16} and ν_{17}, in both the Raman spectrum and the infrared spectrum. For ν_{18}, as for the gauche rotamers of the other two isotopomers, we interpret the broad shoulder in the infrared spectrum at about 240 cm^{-1} and a weak depolarized band in the Raman spectrum at 240 cm^{-1} as evidence for ν_{18}. A very weak, apparently depolarized Raman band at about 991 cm^{-1} is a possibility for ν_{13}. The weak feature at 980 cm^{-1} remains at −100 °C and thus is assigned to a combination tone of the anti rotamer. The B-like band at 1204 cm^{-1} in the infrared spectrum is a reasonable candidate for ν_{14} because it loses intensity as the temperature is decreased. No spectral evidence was found for the other two fundamentals of the b symmetry species.

As shown in Table 4, the assignment of fundamentals for the gauche rotamer of the d_2 species is as incomplete as the assignment for the $^{13}C_2$ species. This incompleteness is in contrast to the anti rotamer of the d_2 species for which the strongest evidence exists for a complete assignment. Supplementary Table S3 gives the details of the observations and assignments of all the spectral features for the d_2 isotopomer.

Conclusions

An efficient method has been developed for synthesizing small amounts of the $^{13}C_2$ and d_2 isotopomers of TFEA by preparing isotopically substituted TBrEA from acetylene-$^{13}C_2$ and acetylene-d_2 and then reacting the substituted TBrEA with AgF_2. Intermediates and products have been characterized.

The published assignments of vibrational fundamentals for the rotamers of the normal form of TFEA have been revised. High-resolution, gas-phase infrared spectra at low temperature from the work of Stone et al. and from Giessen, though fragmentary, helped considerably. For the anti rotamer two adjustments have been made based on the new infrared spectral evidence. For the gauche rotamer, seven adjustments have been made in assignments of fundamentals, and estimates for the missing ones are proposed. Several of the revisions were dependent on the calculations of frequencies and infrared intensities reported by Kenny et al. The assignments for the two rotamers of the normal form are in Tables 2 and 4. Assignments of the fundamentals of both rotamers of TFEA have undergone a remarkably large change since the initial, extensive investigation of Klaboe and Nielsen. Nine fundamentals for the anti rotamer and eight for the gauche rotamer have been revised.

Turning to a closer comparison of the observed and calculated frequencies for the rotamers of the normal species, we see that, as commonly found, the observed values are smaller than the calculated values with some exceptions at low frequencies. A simple scaling rule for adjusting the calculated frequencies is insufficient. A better procedure is to recognize that the differences between calculated and observed frequencies are approximately equal for fundamentals of similar normal modes. In this way, the expected values for ν_5, ν_{10}, and ν_{14} are estimated as 1100, 75, and 1135 cm^{-1}, respectively, for the gauche rotamer of the normal species.

Based on infrared and Raman spectral evidence, assignments of fundamentals are proposed for both rotamers of the $^{13}C_2$ and d_2 isotopomers. For the two anti rotamers of the isotopomers the assignments are complete. For all three isotopomers, the occurrence of only the anti rotamer in crystalline material guides the assignments for this rotamer, which are summarized in Table 2. The assignments for the anti rotamers of the three isotopomers are consistent with Teller−Redlich product rule ratios.

For the less abundant gauche rotamers of the three isotopomers, the identification of the vibrational fundamentals remains incomplete. Dominance of spectral regions by bands of the more abundant anti rotamer coupled with the absence of a way to observe bands of the gauche rotamer alone compromise the experimental evidence for the fundamentals of the gauche rotamer. The assignments for the fundamentals of the gauche rotamers of the three isotopomers are summarized in Table 4. Frequencies in brackets for the normal species are estimates. In the absence of ab initio calculations for the $^{13}C_2$ and d_2 isotopomers, good estimates cannot be made for the missing frequencies for these species.

Because the assignments of the fundamentals of the anti rotamers of the three isotopomers are well supported by experimental observations and calculations, a firm foundation exists for the investigation of the complete structure of the anti

rotamer of TFEA by high-resolution infrared spectroscopy. Further clarification of the assignment of fundamentals for the gauche rotamer awaits a study of the high-resolution infrared spectra for the gas phase over the whole spectral range at low temperature.

Acknowledgment. This research was supported by National Science Foundation grant CHE 9710375 and by Oberlin College. We are grateful to Dr. Michael Lock at Justus Liebig University in Giessen, Germany for recording the high-resolution infrared spectra and to Joshua B. Burton for his contributions to the development of the synthetic method.

Supporting Information Available: Tables S1−S3 contain details of the spectra and assignments for each of the isotopic species of TFEA. This material is available free of charge via the Internet at http://pubs.acs.org.

References and Notes

(1) Durig, J. R.; Liu, J.; Little, T. S.; Kalasinsky, V. F. *J. Phys. Chem.* **1992**, *96*, 8224.

(2) Craig, N. C.; Chen, A.; Suh, K.-H.; Klee, S.; Mellau, G. C.; Winnewisser, B. P.; Winnewisser, M. *J. Phys. Chem. A* **1997**, *101*, 9302.

(3) Muir, M.; Baker, J. *Mol. Phys.* **1996**, *89*, 211.

(4) Wiberg, K. B. *Acct. Chem. Res.* **1996**, *29*, 229.

(5) Engkvist, O.; Kalstrom, G.; Widmark, P.-O. *Chem. Phys. Lett.* **1997**, *265*, 19.

(6) Kalasinsky, V. F.; Anjaria, H. V.; Little, T. S. *J. Phys. Chem.* **1982**, *86*, 1351.

(7) Papasavva, S.; Illinger, K. H.; Kenny, J. E. *J. Phys. Chem.* **1996**, *100*, 10 100.

(8) Epiotis, N. D. *Deciphering the Chemical Code. Bonding Across the Periodic Table*; VCH Publishers: New York, 1996; Chapter 11.

(9) Takeo, H.; Matsumura, C.; Morino, Y. *J. Chem. Phys.* **1986**, *84*, 4205.

(10) Stone, S. C.; Philips, L. A.; Fraser, G. T.; Lovas, F. J.; Xu, L.-H.; Sharpe, S. W. *J. Mol. Spectrosc.* **1998**, *192*, 75.

(11) Klaboe, P.; Nielsen, J. R. *J. Chem. Phys.* **1960**, *32*, 899.

(12) Chen, Y.; Paddison, S. J.; Tschuikow-Roux, E. *J. Phys. Chem.* **1994**, *98*, 1100.

(13) Henne, A. L.; Midgley, T. *J. Am. Chem. Soc.* **1936**, *58*, 884.

(14) Smith, K.; Newnham, D.; Page, M.; Ballard, J.; Duxbury, G. *J. Quant. Spectrosc. Radiat. Transfer* **1998**, *59*, 437.

(15) Becker, E. D. *High-Resolution NMR, Theory and Chemical Applications*, 2nd ed.; Academic Press: New York, 1980.

(16) Cavalli, L.; Abraham, R. J. *Mol. Phys.* **1970**, *19*, 265.

(17) Ackermann, M. N.; Burdge, J. J.; Craig, N. C. *J. Chem. Phys.* **1973**, *58*, 203.

(18) Calculated with the energy differences reported in ref 6 and assuming $\Delta_r S^\circ = R \ln 2$ for the anti-to-gauche conversion. The two rotamers have the same rotational symmetry number (2), and the gauche has weight 2 because of two forms of this rotamer. For the gas phase, $\Delta_r H^\circ = 4.94$ kJ/mol; for the liquid phase, $\Delta_r H^\circ = 1.51$ kJ/mol.